Bacillus anthracis o-Succinylbenzoyl-CoA Synthetase: Reaction Kinetics and a Novel Inhibitor Mimicking Its Reaction Intermediate†

Yang Tian,‡ Dae-Hwan Suk,§,|| Feng Cai,§,⊥ David Crich,§,⊥ and Andrew D. Mesecar*,‡

Center for Pharmaceutical Biotechnology, Department of Medicinal Chemistry and Pharmacognosy, University of Illinois, 900 South Ashland Avenue, Chicago, Illinois 60607, and Department of Chemistry, University of Illinois, 845 West Taylor Street, Chicago, Illinois 60607

Received July 11, 2008; Revised Manuscript Received October 2, 2008

ABSTRACT: *o*-Succinylbenzoyl-CoA (OSB-CoA) synthetase (EC 6.2.1.26) catalyzes the ATP-dependent condensation of *o*-succinylbenzoate (OSB) and CoA to form OSB-CoA, the fourth step of the menaquinone biosynthetic pathway in *Bacillus anthracis*. Gene knockout studies have highlighted this enzyme as a potential target for the discovery of new antibiotics. Here we report the first studies on the kinetic mechanism of *B. anthracis* OSB-CoA synthetase, classifying it as an ordered bi uni uni bi ping-pong mechanism. Through a series of pre-steady-state and steady-state kinetic studies in conjunction with direct binding studies, it is demonstrated that CoA, the last substrate to bind, strongly activates the first half-reaction after the first round of turnover. The activation of the first half-reaction is most likely achieved by CoA stabilizing conformations of the enzyme in the "F" form, which slowly isomerize back to the E form. Thus, the kinetic mechanism of OSB-CoA synthetase may be more accurately described as an ordered bi uni uni bi iso ping-pong mechanism. The substrate specificity of OSB-CoA synthetase was probed using a series of OSB analogues with alterations in the carboxylate groups. OSB-CoA shows a strong preference for OSB over all of the analogues tested as none were active except 4-[2-(trifluoromethyl)phenyl]-4-oxobutyric acid which exhibited a 100-fold decrease in k_{cat}/K_m. On the basis of an understanding of OSB-CoA synthetase's kinetic mechanism and substrate specificity, a reaction intermediate analogue of OSB-AMP, 5′-*O*-{*N*-[2-(trifluoromethyl)phenyl]-4-oxobutyl}adenosine sulfonamide (TFMP-butyl-AMS), was designed and synthesized. This inhibitor was found to be an uncompetitive inhibitor to CoA and a mixed-type inhibitor to ATP and OSB with low micromolar inhibition constants. Collectively, these results should serve as an important forerunner to more detailed and extensive inhibitor design studies aimed at developing lead compounds against the OSB-CoA synthetase class of enzymes.

The bacterial menaquinone biosynthetic enzymes are potentially attractive targets for the discovery of antibiotics because they are essential for bacterial growth and are absent from humans. Menaquinone is an essential lipophilic molecule that shuttles electrons between dehydrogenases and cytochromes in the bacterial electron transport chain (*1*). Members of the *Bacillus* family of bacteria cannot acquire menaquinone from the environment and therefore require the menaquinone biosynthetic pathway for the production of this critical cofactor (*1, 2*). Studies on *Bacillus subtilis* have demonstrated that deletion of any of its menaquinone biosynthetic genes compromises its growth in LB medium (*3*). Although knockout studies on the menaquinone biosynthetic genes from *Bacillus anthracis* have not yet been reported, by analogy it is possible that these genes are also essential for growth of *B. anthracis* since it is a close relative of *B. subtilis* (*4*). Finally, since the entire bacterial menaquinone biosynthetic pathway is absent from the human genome as humans utilize ubiquinone for the electron transport chain in the mitochondria, the enzymes in the menaquinone pathway are unique and therefore attractive targets for the discovery of new antibiotics against *B. anthracis* and other bacteria.

Among all the *B. anthracis* menaquinone biosynthetic enzymes, *o*-succinylbenzoyl-coenzyme A (OSB-CoA)[1] synthetase was chosen as a potential drug target of our studies on the basis of the availability of various assays for detection of the enzymatic reaction products (*5, 6*), and the fact that the substrate OSB and various analogues can be readily obtained by chemical synthesis (*7*). OSB-CoA synthetase (EC 6.2.1.26) catalyzes the fourth reaction in the menaquinone biosynthetic pathway that converts the substrates OSB, ATP,

† This research is supported by a Grant AI056575 from the National Institutes of Health, National Institute of Allergy and Infectious Diseases.

* To whom correspondence should be addressed. Phone: (312) 996-1877. Fax: (312) 413-9303. E-mail: mesecar@uic.edu.

‡ Department of Medicinal Chemistry and Pharmacognosy.

§ Department of Chemistry.

|| Current address: Center for Bioactive Molecular Hybrids and Department of Chemistry, Yonsei University, Seoul 120-749, Korea.

⊥ Current address: Department of Chemistry, Wayne State University, 5101 Cass Ave., Detroit, MI 48202.

[1] Abbreviations: OSB, *o*-succinylbenzoate; OSB-CoA, *o*-succinylbenzoyl-coenzyme A; TFMP-butyl-AMS, 5′-*O*-{*N*-[2-(trifluoromethyl)phenyl]-4-oxobutyl}adenosine sulfonamide; IPP, inorganic pyrophosphatase; PNP, purine nucleoside phosphorylase; MESG, 2-amino-6-mercapto-7-methylpurine ribonucleoside; IPTG, isopropyl β-D-thiogalactopyranoside.

10.1021/bi801311d CCC: $40.75
Published on Web 10/31/2008

Scheme 1

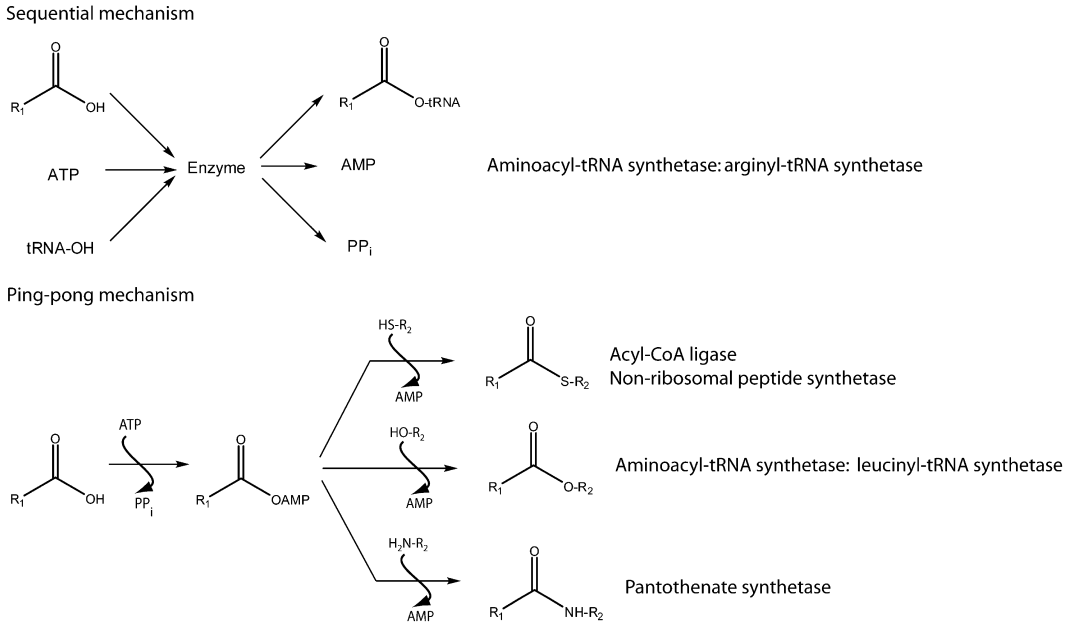

and CoA to the products AMP, PP_i, and OSB-CoA (*8*). Mg^{2+} is also required for the enzymatic activity (*9, 10*). Enzymes using ter-reactant mechanisms usually catalyze either a ter-ter sequential reaction (*11*) or a bi uni uni bi ping-pong reaction (*12*−*15*) (Scheme 1). *Escherichia coli* arginyl-tRNA synthetase utilizes a ter-ter sequential mechanism for its reaction whereby all three substrates (ATP, arginine, and tRNA) must bind to the enzyme before any of the three products (PP_i, AMP, and arinyl-tRNA) are released into the bulk solution (*11*). In contrast, other enzymes follow a bi uni uni bi ping-pong reaction with the formation of an acyl-AMP intermediate (*12*−*15*). As illustrated in Scheme 1, the reaction proceeds in two steps. In the first step, a carboxylic acid substrate reacts with ATP to form an acyl-AMP intermediate and release the first product, PP_i. In the second step, the acyl-AMP intermediate reacts with the third substrate to form the last two products. In this case, the third substrate is not required for the first step of the reaction. As expected, the formation of an acyl-AMP intermediate has been experimentally confirmed in the enzymes that utilize ping-pong reaction mechanisms but not in the enzymes utilizing sequential mechanisms (*14*−*17*). Indeed, analogues that mimic the reaction intermediate have been found to be potent inhibitors of the enzymes that follow a ping-pong mechanism (*18, 19*).

In a manner analogous to the reaction mechanism mentioned above, OSB-CoA synthetase may catalyze either a ping-pong or a sequential reaction. To determine which kinetic mechanism is utilized by *B. anthracis* OSB-CoA synthetase, the steady-state kinetics of the reaction were studied by initial velocity, product inhibition, and direct binding studies. The pre-steady-state kinetics of the first half-reaction and the overall reaction were also studied, and the substrate specificity of the enzyme was probed using a series of OSB analogues. On the basis of these experimental results, a potent reaction intermediate analogue was designed and synthesized, which is the first potent inhibitor of an OSB-CoA synthetase from any organism.

MATERIALS AND METHODS

Materials. ATP, AMP, CoA, benzoyl-CoA, yeast inorganic pyrophosphatase (IPP), and bacterial purine nucleoside phosphorylase (PNP) were purchased from Sigma (St. Louis, MO). The compound 2-amino-6-mercapto-7-methylpurine ribonucleoside (MESG) was purchased from Berry & Associates (Dexter, MI). Restriction enzymes *Nde*I and *Bam*HI were purchased from Fermentas (Hanover, MD). T4 DNA ligase and *Pfx* DNA polymerase were purchased from Invitrogen Corp. (Carlsbad, CA). Plasmid vector pET15b and *E. coli* strain BL21(DE3) were purchased from Novagen (Madison, WI). All chromatographic instruments and columns were purchased from Amersham Biosciences (Piscataway, NJ).

Chemical Synthesis. OSB, **1**, was synthesized as previously described (*7*). Four OSB analogues, **2**−**5**, and **6**, an OSB-AMP analogue, 5′-*O*-{*N*-[2-(trifluoromethyl)phenyl]-4-oxobutyl}adenosine sulfonamide (TFMP-butyl-AMS), were synthesized, and the procedures are described in the Supporting Information. The structures for these compounds are given in Figure 1.

Cloning, Expression, and Purification of 1,4-Dihydroxy-2-naphthoate-CoA (DHNA-CoA) Synthetase (MenB) from E. coli. The full details for the expression and purification are given in the Supporting Information.

Cloning, Expression, and Purification of OSB-CoA Synthetase from B. anthracis. The *B. anthracis* OSB-CoA synthetase gene (*menE*) sequence was obtained from Genbank accession number BA5108. The *menE* gene was obtained by PCR amplification from genomic DNA isolated from the *B. anthracis* Sterne strain which was a generous gift from A. A. Neyfakh (University of Illinois) using *Pfx* DNA polymerase. Two primers (5′-GACACGACATATG-GAGACGATGCCAAATTGGTTA-3′ and 5′-CGGGATC-CTTACATCTCCTCCACTAATTGTCTTAACTCTCG-3′) containing *Nde*I and *Bam*HI sites (underlined in the primer sequences) were used for the PCRs. The PCR products were cloned into the pET15b plasmid using the two restriction

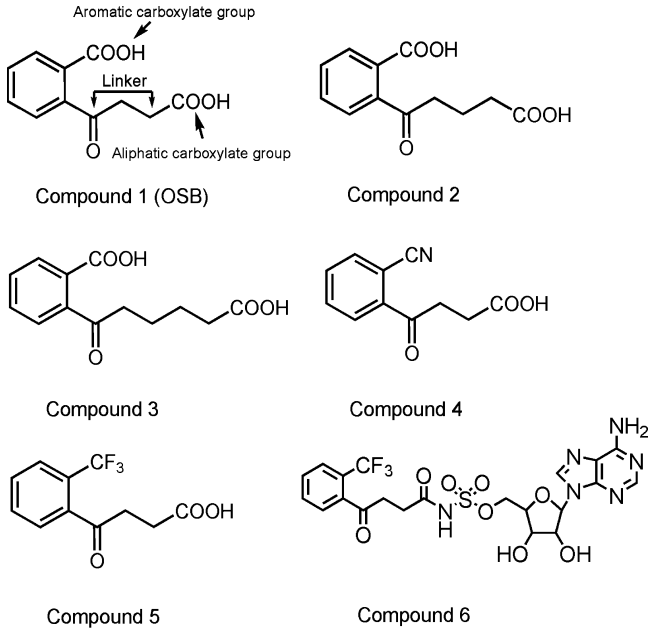

FIGURE 1: Structures of OSB, OSB analogues, and an OSB-AMP analogue. Compound **6** (TFMP-butyl-AMS) is an OSB-AMP analogue that was designed and synthesized by covalently linking compound **5** and a sulfonamide adenosine. Synthetic protocols for these compounds are given in the Supporting Information.

sites mentioned above which placed the *menE* gene in frame with an N-terminal $(His)_6$ tag sequence. The entire *menE* gene was sequenced at the DNA sequencing facility at the Research Resource Center (RRC) of the University of Illinois. The mutation-free construct was transformed into *E. coli* strain BL21(DE3) for expression. Cells were grown at 37 °C in 4 L of LB medium until the OD_{600} reached 0.6, when IPTG was added to the cell culture at a final concentration of 0.1 mM for induction of protein expression. After being induced for 2 h, cells were collected by centrifugation at 3300*g* for 10 min at 4 °C. For purification, 12 g of cell pellet was resuspended in 30 mL of buffer A [50 mM Tris-HCl, 10 mM imidazole, and 0.5 M NaCl (pH 7.5)] and lysed by sonication using a GEX-600 sonics ultrasonic processor (Sonics and Materials, Inc., Newtown, CT) with a 0.5 in. probe. The sonication lasted for 6 min with a repeating pulse of 6.6 s on and 9.9 s off at 65% amplitude. The cell lysate was centrifuged at 39000*g* for 40 min at 4 °C, after which the supernatant was collected and filtered through a 0.22 μm filter (Millipore, Carrigtwohill, County Cork, Ireland). The clear filtrate (~30 mL) was loaded onto a 5 mL HiTrap affinity column (1.6 cm × 2.5 cm) (Amersham Biosciences) charged with cobalt and equilibrated with buffer A. The column was washed with 100 mL of buffer A to remove any weakly bound proteins. OSB-CoA synthetase was then eluted using a linear gradient from 0 to 100% buffer B [50 mM Tris-HCl, 1 M imidazole, and 0.5 M NaCl (pH 7.5)] for 120 mL. Fractions containing OSB-CoA synthetase were pooled, and 3.8 M ammonium sulfate was added to a final concentration of 1 M. The resulting solution was loaded on a HP Phenyl Sepharose column (1.6 cm × 20 cm) (Amersham Biosciences) equilibrated with buffer C [50 mM Tris-HCl, 1 M ammonium sulfate, and 0.2 M NaCl (pH 7.5)]. The column was washed with 200 mL of buffer C to remove weakly bound proteins. OSB-CoA synthetase was eluted using a linear gradient from 0 to 100% buffer D [50 mM Tris-HCl and 0.1 M NaCl (pH 7.5)]. Fractions were analyzed by SDS−PAGE, and those containing pure OSB-CoA synthetase were pooled. Prior to storage at −80 °C, the buffer was exchanged with 50 mM Tris-HCl (pH 7.5), and the protein was concentrated to ~100 μM using a protein concentrator (Millipore). Protein concentrations were determined using a Bio-Rad protein assay kit (Bio-Rad Laboratories Inc., Hercules, CA) with bovine serum albumin (BSA) as a standard.

OSB-CoA Synthetase Activity Assay. Two assays were utilized for the measurement of OSB-CA synthetase activity. In the first assay (see Figure S1a of the Supporting Information), the release of PP_i was coupled to the reactions of IPP and PNP as previously described (*5*). The increase in the absorbance of 2-amino-6-mercapto-7-methylpurine at 360 nm was monitored on a SpectraMax 384 Plus plate reader (Molecular Devices, Sunnyvale, CA). A molar extinction coefficient of 11000 M^{-1} cm^{-1} was used to calculate the amount of product formed. The assays were performed in 96-well plate format with an assay volume of 200 μL. Each assay contained 50 mM Tris-HCl, 20 mM NaCl, 2 mM $MgCl_2$, 0.5 unit of PNP, 0.075 unit of IPP, 300 μM MESG (pH 7.5), and different concentrations of OSB, ATP, and CoA. This reaction mixture was preincubated for 10 min, and the reaction was initiated with a final concentration of OSB-CoA synthetase of 50 nM. The reaction rates were obtained from the initial, linear region of the reaction progress curves. A unit of enzyme activity is defined as 1 μmol of PP_i formed per minute with the specific activity defined as one unit per milligram of enzyme. All assays were performed at 21 °C. The assay conditions described above were used throughout this report, unless specified otherwise.

In the second assay (see Figure S1b of the Supporting Information), OSB-CoA synthetase activity was measured by coupling the formation of the product, OSB-CoA, to the reaction catalyzed by DHNA-CoA synthetase (*20*). In this reaction, OSB-CoA is converted into DHNA-CoA which has a molar extinction coefficient of 4000 M^{-1} cm^{-1} at 392 nm (*20*). For the 96-well, plate-based assay, a 200 μL standard assay mixture contained 50 mM Tris-HCl, 20 mM NaCl, 2 mM $MgCl_2$, 88 μM *E. coli* DHNA-CoA synthetase (pH 7.5), and varying concentrations of OSB, ATP, and CoA. The reaction was initiated by the addition of OSB-CoA synthetase to a final concentration of 1 μM. The reaction rates were determined from the initial linear region of the reaction progress curve. One unit of activity is defined 1 μmol of DHNA-CoA formed per minute.

Single-Substrate Kinetics of B. anthracis OSB-CoA Synthetase. The K_m and k_{cat} values for each of the three substrates (OSB, ATP, and CoA) were determined by single-substrate kinetics. The first set of enzyme reaction rate measurements were taken by varying the OSB concentration (from 1 to 256 μM) and fixing the ATP (512 μM) and CoA (1024 μM) concentrations. For the second set of initial velocity measurements, the ATP concentration was varied (from 2 to 512 μM) at fixed OSB (256 μM) and CoA (1024 μM) concentrations. For the third set of initial velocity measurements, the CoA concentration was varied (from 8 to 1024 μM) at fixed OSB (256 μM) and ATP (512 μM) concentrations. Finally, a kinetic study for the OSB analogue (compound **5** in Figure 1) was performed by varying the concentration of **5** from

12 to 3000 μM and fixing the ATP (512 μM) and CoA (1024 μM) concentrations. The data were fit to eq 1:

$$v = V_{max}[S]/(K_m + [S]) \quad \text{(Michaelis−Menten)} \qquad (1)$$

where v is the reaction rate (micromoles per minute per milligram), V_{max} is the maximum reaction rate (micromoles per minute per milligram), [S] is the varying substrate or substrate analogue concentration (micromolar), and K_m is the Michaelis−Menten constant. The data were fit to eq 1 using the Enzyme Kinetics module in SigmaPlot 2000 (SYSTAT Software, Inc., Point Richmond, CA).

Initial Velocity Studies. Bisubstrate kinetic studies were performed for the initial velocity study. The reaction rates were studied by varying the concentrations of two substrates in the presence of a fixed, variable concentration of the third substrate. The experimental data were fit to eqs 2−5 using nonlinear regression analysis. The goodness of fit was evaluated on the basis of the Akaike Information Criterion corrected for small sample size (AIC_c) values and the standard errors of the parameter estimates (*21*). AICc is used for comparing non-nested enzyme kinetic equations. AICc improves the performance of AIC when the sample size is small compared to the number of equation parameters. The equation with the lower or more negative AICc value is considered to be the equation that best fits the data set. A difference of ≥7 in the AICc values is considered to be statistically significant in distinguishing between models (*21*). If two the equations have nearly the same AICc values or the differences between their AICc values are less than 7, AICc values alone cannot be used to distinguish between models. In such cases, the equation with the better estimate of the fitted parameters and with a random distribution of residuals in residual plots can be classified as the better fit and to infer the more appropriate kinetic model. The kinetic mechanism and relevant kinetic parameters were derived from a best fit to one of the following equations:

$$v = V_{max}[A][B]/(K_{mA}[B] + K_{mB}[A] + [A][B]) \quad \text{ping-pong} \qquad (2)$$

$$v = V_{max}[A][B]/(K_aK_b + K_b[A] + [A][B]) \quad \text{rapid-equilibrium ordered} \qquad (3)$$

$$v = V_{max}[A][B]/(K_aK_{mB} + K_{mB}[A] + K_{mA}[B] + [A][B]) \quad \text{steady-state ordered} \qquad (4)$$

$$v = V_{max}[A][B]/(aK_aK_b + aK_a[A] + aK_a[B] + [A][B]) \quad \text{rapid-equilibrium random} \qquad (5)$$

In each of the equations, v is the reaction rate (micromoles per minute per milligram), V_{max} is the maximum velocity of the reaction (micromoles per minute per milligram), [A] is the substrate A concentration (micromolar), [B] is the substrate B concentration (micromolar), K_a and K_b are dissociation constants of substrates A and B (micromolar), respectively, and K_{mA} and K_{mB} are Michaelis−Menten constants for substrates A and B (micromolar), respectively. The data were processed using the Enzyme Kinetics module in SigmaPlot 2000 (SYSTAT Software).

Direct Measurements for Binding of ATP, OSB, and CoA to B. anthracis OSB-CoA Synthetase. The dissociation constants (K_d) of ATP, OSB, and CoA from OSB-CoA synthetase were determined by the centrifugal ultrafiltration method (*22, 23*). Prior to the binding studies, the purified enzyme was dialyzed (40000-fold) in a buffer containing 50 mM Tris-HCl and 20 mM NaCl (pH 7.5) to remove any trace amount of endogenous ligands associated with the enzyme during expression and purification. The binding studies were performed using the same buffer conditions at 21 °C. For the ATP to OSB-CoA synthetase binding study, the enzyme (70 μM) was incubated with increasing concentrations of ATP (from 0 to 800 μM) in the presence and absence of 2 mM $MgCl_2$. For the OSB to OSB-CoA synthetase binding study, the enzyme (70 μM) was incubated with increasing concentrations of OSB (0−800 μM) and 2 mM $MgCl_2$. For the CoA to enzyme binding study, the enzyme (200 μM) was incubated with different concentrations of CoA (0−1280 μM) and 2 mM $MgCl_2$ in the presence and absence of 2 mM ATP. After binding and equilibration for 20 min, the free substrates were separated from the bound substrates by passing ~60 μL of the 500 μL binding mixture through a Microcon YM-10 centrifugal filter device (Millipore Corp., Bedford, MA). The free ATP concentration was determined directly by measuring the absorbance of the filtrate at 260 nm and then extrapolating the concentration values from an ATP concentration versus absorbance standard curve. The concentration of free OSB in the filtrate was measured enzymatically by the phosphate detection assay in the presence of a saturating concentration of ATP (512 μM) and CoA (1024 μM). The increase in absorbance at 360 nm was converted into the concentration of OSB in the filtrate using a molar extinction coefficient of 11000 M^{-1} cm^{-1}. The free CoA concentration was determined by reacting CoA directly with 5,5′-dithiobis-2-nitrobenzoic acid (DTNB). Briefly, equal volumes of filtrate and a DTNB stock solution (4 mM) were mixed, and the absorbance was read at 412 nm. A standard curve of free CoA concentration versus absorbance at 412 nm was constructed and used to obtain the CoA concentration in the filtrates. The fraction of binding v was calculated on the basis of eq 6, and the data were fit to eq 7 for the determination of K_d (*23*):

$$v = ([L]_t - [L]_f)/[E]_t \qquad (6)$$

$$v = V_{max}/[1 + (K_m/[S])(1 + [I]/K_i)] \qquad (7)$$

where $[L]_t$ is the total substrate concentration in the binding assay (micromolar), $[L]_f$ is the free substrate concentration in the filtrate (micromolar), $[E]_t$ is the total OSB-CoA synthetase concentration (micromolar), v is the fraction of binding, and K_d is the dissociation constant of the substrate to the enzyme (micromolar).

Product Inhibition Study. The product inhibition studies were performed with AMP, benzoyl-CoA, and TFMP-butyl-AMS. Benzoyl-CoA was used as a mimic to the product OSB-CoA since the latter compound is not stable (*10*). The effects of these inhibitors on reaction rates were studied by varying the concentration of one product inhibitor and one substrate while keeping the other two substrates at constant subsaturating concentrations. The experimental data were fit to eqs 8−11 by nonlinear regression analysis. The goodness of fit was evaluated on the basis of standard errors of the parameter estimates and AIC_c values. The kinetic mechanism and relevant kinetic parameters were derived from the best fit to one of the following equations: eq 8 for competitive inhibition, eq 9 for uncompetitive inhibition, eq 10 for mixed-type inhibition, and eq 11 for noncompetitive inhibition.

$$v = V_{max}/[1 + (K_m/[S])(1 + [I]/K_i)] \quad \text{competitive inhibition} \quad (8)$$

$$v = V_{max}/(1 + [I]/K_i + K_m/[S]) \quad \text{uncompetitive inhibition} \quad (9)$$

$$v = V_{max}/[(K_m/[S])(1 + [I]/K_i) + 1 + [I]/\alpha K_i] \quad \text{mixed-type inhibition} \quad (10)$$

$$v = V_{max}/[(1 + [I]/K_i)(1 + K_m/[S])] \quad \text{noncompetitive inhibition} \quad (11)$$

In each of the equations, v is the reaction rate (micromoles per minute per milligram), V_{max} is the maximum velocity of the reaction (micromoles per minute per milligram), [S] is the substrate S concentration (micromolar), [I] is the inhibitor I concentration (micromolar), K_m is the Michaelis−Menten constant for substrate S, K_i is the dissociation constant of the inhibitor I to free enzyme E (millimolar), and αK_i is the dissociation constant for inhibitor I to ES complex (millimolar). The data were fit to the equations described above using the Enzyme Kinetics module in SigmaPlot 2000 (SYSTAT Software).

Pre-Steady-State Kinetics of the Enzyme with ATP and OSB. The phosphate detection assay was used to study the pre-steady-state reaction kinetics of OSB-CoA synthetase with the substrates ATP and OSB. The assays were performed in a 100 μL quartz cuvette with 1 cm path length. The assay contained 50 mM Tris-HCl, 20 mM NaCl, 2 mM $MgCl_2$, 0.5 unit of PNP, 0.075 unit of IPP, 300 μM MESG (pH 7.5), 256 μM OSB, and 512 μM ATP. The reactions were initiated with various concentrations of the enzyme (2.2, 4.4, and 8.8 μM), and the absorbance change at 360 nm was monitored for 2.5 min on a Cary 50 Bio UV−visible spectrophotometer (Varian, Inc., Palo Alto, CA). The enzyme concentrations were kept high in this experiment so that the product, PP_i, from a single enzyme turnover could be detected and quantitated. The amount of PP_i formed (micromolar) over time (minutes) was calculated using a molar extinction coefficient of 11000 M^{-1} cm^{-1}. The time course data were fit to eq 12, which describes a single exponential followed by a linear steady-state component (*24*):

$$y = A[1 - \exp(-k_1 t)] + K_2 t \quad (12)$$

where y is the concentration of PP_i released (micromolar), t is the time (minutes), A is the observed burst amplitude (micromolar), k_1 is the observed exponential burst rate constant (inverse minutes), and k_2 is the observed linear steady-state rate (micromolar per minute)

Pre-Steady-State Kinetics of the Enzyme with ATP, OSB, and CoA. The phosphate detection assay was used to study the pre-steady-state reaction kinetics of OSB-CoA synthetase with the substrates ATP, OSB, and CoA. The assays were performed in a 100 μL quartz cuvette with a 1.0 cm path length. The first assay contained 50 mM Tris-HCl, 20 mM NaCl, 2 mM $MgCl_2$, 2.5 units of PNP, 1 unit of IPP, 300 μM MESG (pH 7.5), 256 μM OSB, 512 μM ATP, and 1024 μM CoA. The reactions were initiated with 1 μM OSB-CoA synthetase, and the absorbance change at 360 nm was monitored for 0.4 min on a Cary 50 Bio UV−visible spectrophotometer (Varian, Inc.). The amount of excess coupling enzyme necessary in this assay was determined to ensure that the rate-determining step of the coupled assay was the OSB-CoA synthetase-catalyzed reaction. The amount of PP_i formed (micromolar) over time (minutes) was calculated using a molar extinction coefficient of 11000 M^{-1} cm^{-1}. In the second assay, the OSB-CoA synthetase (1 μM) was preincubated with 50 mM Tris-HCl, 20 mM NaCl, 2 mM $MgCl_2$, 2.5 units of PNP, 1 unit of IPP, 300 μM MESG (pH 7.5), 256 μM OSB, and 512 μM ATP for 1 min so that the steady-state reaction was achieved. An amount of 1024 μM CoA (final concentration) was then added to the reaction mixture, and the absorbance at 360 nm was monitored for 0.4 min.

RESULTS

Single-Substrate Kinetics of B. anthracis OSB-CoA Synthetase. The release of PP_i from the OSB-CoA synthetase reaction was coupled to the reactions of IPP and PNP, resulting in an increase in the absorbance at 360 nm. Using this pyrophosphate detection assay, the purified enzyme exhibited maximal activity between pH 7.25 and 7.5 (Figure S2 of the Supporting Information). As a result, all the experimental studies were performed at pH 7.5. The divalent metal Mg^{2+} was found to be required for enzyme activity and exhibited maximal activities between 1 and 2 mM Mg^{2+} (Table S1 of the Supporting Information). A total Mg^{2+} concentration of 2 mM was used therefore throughout the studies. To determine the initial estimates of the values for the kinetic parameters of OSB, ATP, and CoA, we performed a single-substrate kinetic study by varying one substrate concentration and fixing the other two substrate concentrations. The single-substrate kinetic parameters are listed in Table 1. CoA showed the highest K_m values of the three substrates, while ATP and OSB exhibited similar K_m values. The enzyme has k_{cat} values in the range of ~155 min^{-1}.

Table 1: Kinetic Parameters and Patterns for *B. anthracis* OSB-CoA Synthetase from the Single-Substrate and Bisubstrate Initial Velocity Studies[a]

fixed concentration (μM)			apparent K_m (μM)				
OSB	ATP	CoA	OSB	ATP	CoA	k_{cat} (min^{-1})	k_{cat}/K_m ($min^{-1}\mu M^{-1}$) or kinetic patterns
−	512	1024	21.9 ± 2.0	−	−	155 ± 3.6	7.1
256	−	1024	−	26.8 ± 2.7	−	153 ± 3.2	5.7
256	512	−	−	−	304 ± 22.1	156 ± 4.5	0.5
8	−	−	−	19.3 ± 1.3	231 ± 18.4	80.7 ± 2.7	ping-pong
64	−	−	−	10.6 ± 0.7	279 ± 19.3	108 ± 3.3	ping-pong
−	8	−	12.8 ± 0.8	−	194 ± 14.9	63.6 ± 2.1	ping-pong
−	128	−	5.8 ± 0.5	−	269 ± 24.9	66.1 ± 4.5	ping-pong
−	−	256	1.5 ± 0.2	3.2 ± 0.5	−	52.7 ± 0.8	sequential
−	−	1024	5.0 ± 0.9	8.7 ± 0.9	−	80.0 ± 1.9	sequential

[a] Data presented as means ± the standard error in the fit parameters.

Using the OSB-CoA detection assay, the purified enzyme exhibited a k_{cat} value of 134.0 ± 12.5 min^{-1} for the OSB-CoA release rate. All of the kinetic parameters are comparable to that of *E. coli* OSB-CoA synthetase (*9*).

OSB Substrate Analogues. To probe the contribution of the functional groups of OSB to substrate reactivity, we focused on the modification of the two carboxylate groups of OSB: the aromatic carboxylate group and the aliphatic carboxylate group. Compounds **2** and **3** have linkers for the aliphatic carboxylate group longer than that of OSB (Figure 1). Compounds **4** and **5** have the same aliphatic carboxylate group as OSB, but they have a CN or CF_3 group that replaces the aromatic carboxylate group of OSB (Figure 1). Compounds **2**−**5** were first tested for their ability to serve as substrates for OSB-CoA synthetase. At a concentration of 1 mM for each of the OSB analogues, OSB-CoA synthetase exhibited 5.8% residual activity only toward compound **5** {4-[2-(trifluoromethyl)phenyl]-4-oxobutyric acid} and little to no measurable activity with compounds **2**−**4**. OSB-CoA synthetase has a K_m value of 166 ± 18 μM and a k_{cat} value of 12.5 ± 3.6 min^{-1} for compound **5**. Compared to OSB, OSB-CoA has a significant decrease (100-fold) in rate constant for capture, k_{cap} or k_{cat}/K_m, for compound **5** in addition to a reduced (10-fold) rate constant, k_{rel} or k_{cat}, for its release (*25, 26*).

Initial Velocity Study. To study the order of substrate addition for OSB-CoA synthetase, bisubstrate kinetic studies were performed. The three possible combinations of the variable substrate pairs were first studied at a fixed, unsaturating level of the third substrate. Nonlinear regression was performed on the experimental data using eqs 2−5, and the resulting goodness-of-fit values for each equation are listed in Table S2 of the Supporting Information. When the OSB concentration was fixed at a constant, nearly saturating level (64 μM) and the CoA concentrations were varied at several fixed concentrations of ATP, the data were best fit to eq 2, and the Lineweaver−Burk plot of the data produced a series of parallel lines (Figure 2A). A similar result and plot were also obtained when the ATP concentration was fixed at a constant, nearly saturating level (128 μM), and CoA concentrations were varied at several fixed concentrations of OSB (Figure 2B). The observation of parallel lines in those plots indicated a ping-pong kinetic mechanism in which a chemistry step and transformation of the enzyme into a new enzyme form occur between the addition of the first two substrates (OSB and ATP) and the addition of CoA. On the basis of our observation that the first half-reaction is catalyzed by OSB-CoA synthetase in the absence of CoA (see below), these steps could be the transformation of ATP and OSB into OSB-AMP and PP_i, and the release of PP_i or PP_i and AMP from a ternary enzyme complex. The resulting plots (Figure 2A,B) also indicated that CoA was the final substrate of addition in the kinetic scheme.

When CoA was fixed at a constant, nearly saturating level (1024 μM) and ATP concentrations were varied at several fixed OSB concentrations, the data were best fit to eqs 4 and 5 (eqs 4 and 5 are the same equations but with a different definition of the parameters in the denominator). A Lineweaver−Burk plot of the data produced a series of converging lines (Figure 2C), indicating a sequential mechanism in which there is no product released between the addition of OSB and ATP. Although differentiation between

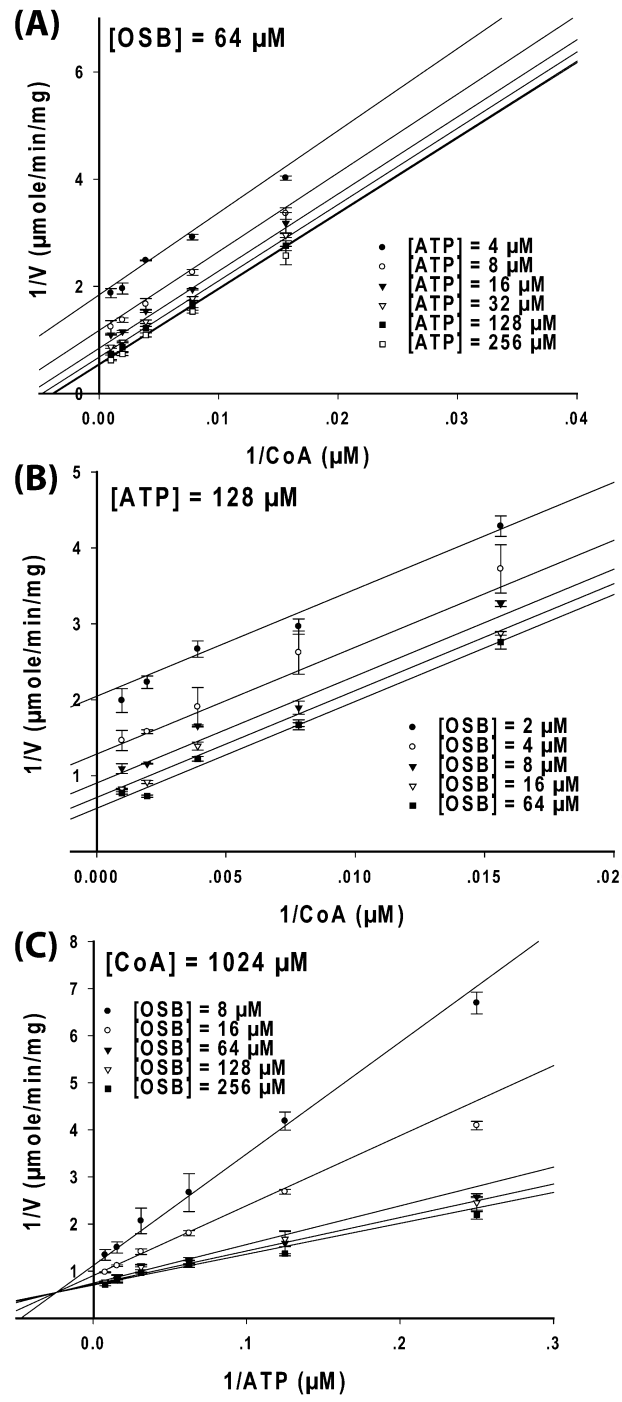

FIGURE 2: Initial velocity study of the *B. anthracis* OSB-CoA synthetase-catalyzed reaction. The kinetic data were displayed as Lineweaver−Burk plots of the reaction rate vs substrate concentrations. For each plot, one substrate was kept at a constant level while the other two substrate concentrations were varied. (A) The OSB concentration was kept constant at 64 μM while the CoA and ATP concentrations were varied: (●) 4, (○) 8, (▼) 16, (▽) 32, (■) 128, and (□) 256 μM. (B) The ATP concentration was kept constant at 128 μM while the CoA and OSB concentrations were varied: (●) 2, (○) 4, (▼) 8, (▽) 16, and (■) 64 μM. (C) The CoA concentration was kept constant at 1024 μM while the ATP and OSB concentrations were varied: (●) 8, (○) 16, (▼) 64, (▽) 128, and (■) 256 μM. Each data point represents the mean of a duplicate test. The upper and lower bars represent the duplicate measurements. The kinetic parameters and patterns are summarized in Table 1.

a steady-state ordered (eq 4) and a rapid-equilibrium random (equation 5) mechanism for the OSB and ATP substrate pair remained unclear solely on the basis of these experiments,

these data did rule out a ter-ter sequential and a hexa-uni ping-pong mechanism and were suggestive of either a bi uni uni bi or bi bi uni uni ping-pong reaction. In both mechanisms, OSB and ATP bind to the free enzyme in a sequential manner, which is then followed by the release of either PP_i or PP_i and AMP before CoA combines with the enzyme.

To support these mechanisms, the kinetic experiments were repeated using 8- and 16-fold decreases (subsaturating) in the concentrations of OSB and ATP. Plots similar to those in panels A and B of Figure 2 were constructed, and parallel lines were also obtained (Figure S3A,B of the Supporting Information). These results further supported the ping-pong mechanism for the OSB/CoA substrate pair and the ATP/CoA substrate pair. Next, the kinetic studies presented in Figure 2C were repeated with a 4-fold decrease in CoA concentration. These data are plotted in Figure S3C of the Supporting Information, and the same pattern of intersecting lines was obtained. Together, the results presented in Figure 2 support a sequential mechanism for the OSB/ATP substrate pair. The initial velocity data were fit to eq 2 (ping-pong mechanism) for the OSB/CoA substrate and ATP/CoA substrate pairs. For the OSB/ATP substrate pair, the data were fit to eq 4 (steady-state ordered mechanism; see below). The kinetic parameters were derived and are summarized in Table 1.

Binding of ATP, OSB, and CoA to OSB-CoA Synthetase. To differentiate between the steady-state ordered and rapid-equilibrium random mechanisms for the OSB and ATP substrate pair, the binding of each substrate to the free enzyme was independently studied by an equilibrium ultrafiltration method. No significant binding of ATP to the free enzyme in the absence of Mg^{2+} was observed (data not shown). However, in the presence of 2 mM Mg^{2+}, a plot of free ATP-Mg^{2+} versus the fractional saturation produced a binding curve with a K_d value of 131 ± 22 μM for ATP-Mg^{2+} (Figure 3A). A Scatchard plot of the binding data indicates a binding ratio of ATP-Mg^{2+} to the free enzyme of 1:1 (Figure 3B).

For the substrate OSB, no significant binding to the free enzyme was observed (Figure 3A) which could result from a high K_d for OSB and therefore a lack of a defined binding site for OSB with the free enzyme. Binding of OSB to the enzyme−Mg^{2+}-ATP complex could not be studied since significant turnover during the incubation period made it difficult to measure the free OSB concentration in the filtrate. On the basis of these direct binding data, an ordered binding mechanism of ATP followed by OSB to the enzyme is suggested. These results rule out a random-sequential mechanism and support an ordered-sequential mechanism for the first half-reaction. Finally, no significant binding of CoA to the free enzyme or to the enzyme−Mg^{2+}-ATP complex was observed (Figure 3A), indicating that CoA must combine with a form of the enzyme generated after the binding of Mg^{2+}-ATP. From this point on, we will refer to Mg^{2+}-ATP as ATP.

Product Inhibition Studies. To differentiate between the bi bi uni uni ping-pong and the bi uni uni bi ping-pong mechanisms and to study the order of product release, we performed product inhibition studies. Nonlinear regression was performed on the experimental data using eqs 8−11, and the resulting goodness-of-fit values are listed in Table S3 of the Supporting Information. When the ATP concentrations were varied at fixed concentrations of AMP with both OSB and CoA concentrations fixed at subsaturating levels, the data fit best to eq 8. A Lineweaver−Burk plot of the data produced a series of lines that converge on the *y*-axis (Figure 4A), indicating AMP is a competitive inhibitor of ATP. This result was consistent with a bi uni uni bi ping-pong mechanism and ruled out the bi bi uni uni ping-pong mechanism. As a result, OSB-CoA and AMP are the last two products to be released (the Q and R products). There were two possible mechanisms for the release of products, random or ordered. When CoA concentrations were varied at fixed concentrations of AMP with both OSB and ATP kept at subsaturating levels, the data were best fit to eq 9 and the Lineweaver−Burk plot produced a series of parallel lines (Figure 4B), indicating AMP is an uncompetitive inhibitor of CoA.

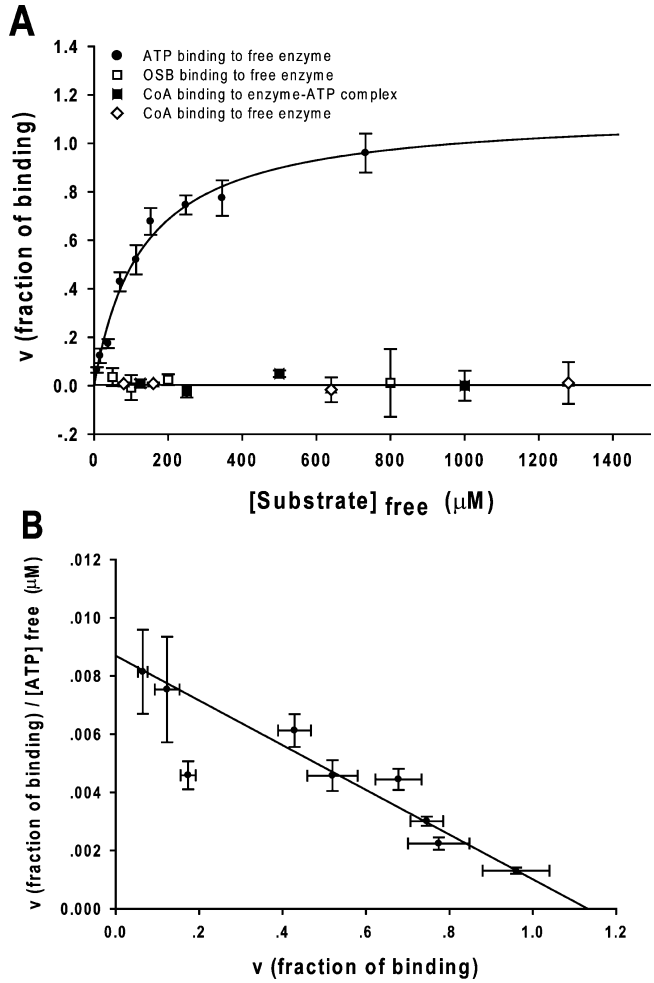

FIGURE 3: Direct binding measurements of the interaction of ATP, OSB, and CoA with *B. anthracis* OSB-CoA synthetase. (A) The binding to ATP (●), OSB (□), and CoA (◇) to the free enzyme and the binding of CoA (■) to the enzyme−ATP complex were assessed using the ultrafiltration method described in Materials and Methods. The resulting binding curve for ATP was obtained by nonlinear regression analysis of the raw data fitting to eq 7. The K_d for binding of ATP to the free enzyme was determined to be 131 ± 23 μM. No significant binding of OSB or CoA to the free enzyme or to the enzyme−ATP complex was observed. Each data point represents the average of four replicates, and the error bars represent the standard deviation of the data at each concentration. (B) Scatchard plot transformation of the ATP binding data shown in panel A. The plot intersects the *x*-axis between 1.0 and 1.2, indicating a binding stoichiomtery of ATP to free enzyme of 1:1.

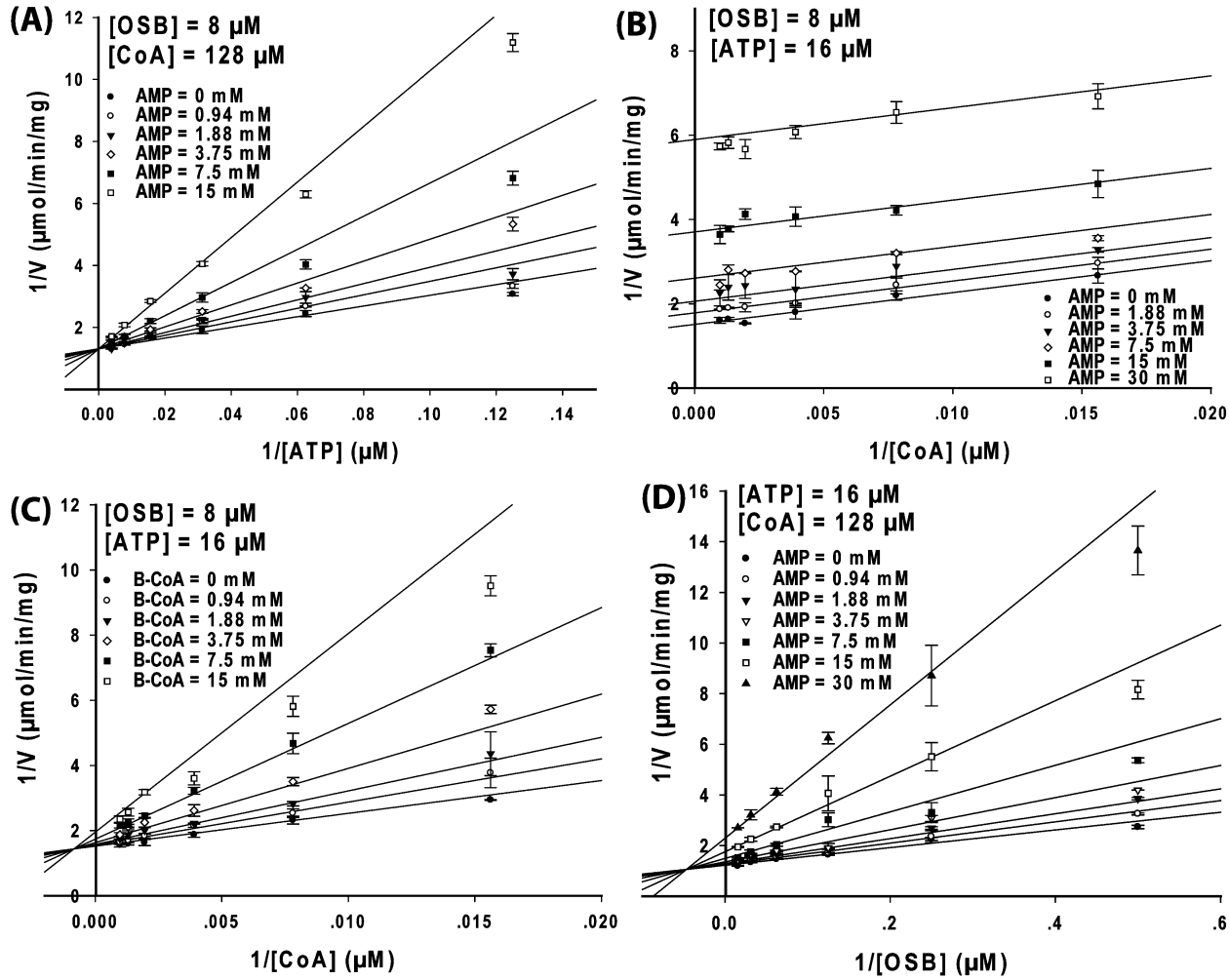

FIGURE 4: Product inhibition study of the *B. anthracis* OSB-CoA synthetase-catalyzed reaction. The kinetic data were displayed as Lineweaver−Burk plots of the reaction rate vs substrate concentrations at different concentrations of the product inhibitor. For each plot, the concentrations of the two substrates were kept at constant level while the third substrate and product inhibitor concentrations were varied. (A) AMP is a competitive inhibitor of ATP. The OSB and CoA concentrations were kept constant at 8 and 128 μM, respectively, while the ATP and AMP concentrations were varied: (●) 0, (○) 0.94, (▼) 1.88, (◇) 3.75, (■) 7.5, and (□) 15.0 mM. The inset is a zoom-out of the region where the lines cross at the *y*-axis. (B) AMP is an uncompetitive inhibitor of CoA. The OSB and ATP concentrations were kept constant at 8 and 16 μM, respectively, while the CoA and AMP concentrations were varied: (●) 0, (○) 1.88, (▼) 3.75, (◇) 7.5, (■) 15.0, and (□) 30.0 mM. (C) Benzoyl-CoA (B-CoA) is a mixed-type inhibitor of CoA. The OSB and ATP concentrations were kept constant at 8 and 16 μM, respectively, while the CoA and benzoyl-CoA concentrations were varied: (●) 0, (○) 0.94, (▼) 1.88, (◇) 3.75, (■) 7.5, and (□) 15.0 mM. (D) AMP is a mixed-type inhibitor of OSB. The CoA and ATP concentrations were kept constant at 128 and 16 μM, respectively, while the OSB and AMP concentrations were varied: (●) 0, (○) 0.94, (▼) 1.88, (◇) 3.75, (■) 7.5, (□) 15.0, and (▲) 30 mM. Each data point represents the mean of a duplicate test. The upper and lower bars represent the duplicate measurements. The kinetic parameters and patterns are summarized in Table 2.

Table 2: Inhibition Kinetic Parameters and Patterns for the Inhibitors of *B. anthracis* OSB-CoA Synthetase[a]

		fixed substrate concentration (μM)						
varied substrate	inhibitor	OSB	ATP	CoA	K_m (μM)	K_i (mM)	αK_i (mM)	inhibition pattern
ATP	AMP	8	−	128	13.1 ± 1.0	3.6 ± 0.4	−	competitive
CoA	AMP	8	16	−	49.9 ± 4.9	−	10.3 ± 0.6	uncompetitive
OSB	AMP	−	16	128	2.8 ± 0.2	4.6 ± 0.6	34.5 ± 4.5	mixed
CoA	benzoyl-CoA	8	16	−	66.2 ± 6.3	3.0 ± 0.5	15.3 ± 2.6	mixed
CoA	TFMP-butyl-AMS	8	16	−	39.3 ± 1.8	−	0.0089 ± 0.0005	uncompetitive
ATP	TFMP-butyl-AMS	8	−	128	5.4 ± 0.5	0.0052 ± 0.0008	0.108 ± 0.017	mixed
OSB	TFMP-butyl-AMS	−	16	128	3.6 ± 0.2	0.0056 ± 0.0008	0.025 ± 0.004	mixed

[a] Data presented as means ± the standard error in the fit parameters.

It has been reported that OSB-CoA is an unstable compound which decomposes spontaneously in solution into a spirodilactone (*10*). To circumvent this problem, we used an OSB-CoA analogue, benzoyl-CoA, as an alternative for the product inhibition studies. When CoA concentrations were varied at fixed concentrations of benzoyl-CoA with both ATP and OSB fixed at subsaturating levels, the data were best fit to eq 10. A Lineweaver−Burk plot of the data produced a series of lines that converged to the left of the *y*-axis (Figure 4C), indicating mixed-type inhibition. These

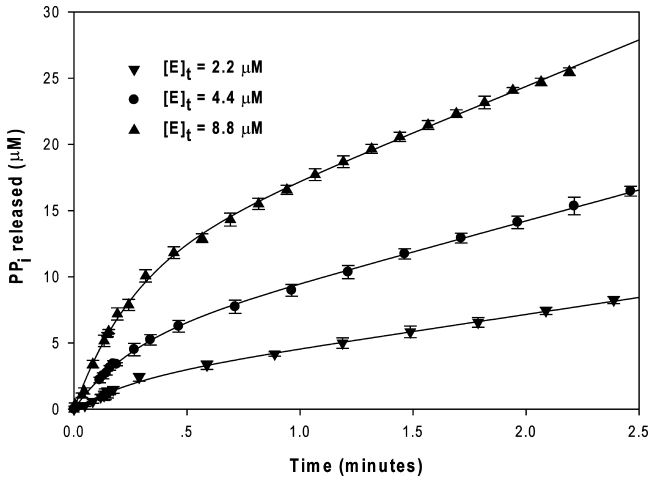

FIGURE 5: Pre-steady-state kinetics of *B. anthracis* OSB-CoA synthetase. The time course of PP_i release was plotted for the presteady state of the first half-reaction (E + ATP + OSB). The reactions were initiated with a final enzyme concentration of 2.2 (▼), 4.4 (●), or 8.8 μM (▲). For clarity, the solid lines of the experimental data were represented by discrete data points. The data from the experiment with E and ATP (control) were subtracted from those from the experiment with E, ATP, and OSB. The data point and error bar represent the average and standard deviation, respectively, of a triplicate measurement. The curves display biphasic stages: a faster burst stage followed by a slower linear stage. The data were fit to eq 12, and the values for the kinetic parameters (burst amplitude, burst rate constant, and linear rate constant) are summarized in Table 3.

results are consistent with an ordered mechanism in which OSB-CoA (the Q product) is released after the addition of CoA and before the release of AMP (the R product). Finally, when OSB concentrations were varied at fixed concentrations of AMP with both ATP and CoA fixed at subsaturating levels, the data were best fit to eq 10 and a Lineweaver−Burk plot of the data produced a series of lines that converged to the left of the *y*-axis (Figure 4D), further supporting the ordered release of OSB-CoA and AMP. The kinetic parameters and product inhibition patterns are summarized in Table 2. AMP and benzoyl-CoA have similar K_i values in the millimolar range, compared to the micromolar range of the K_m values for all three substrates. Thus, the product inhibitors AMP and benzoyl-CoA bind to the enzyme much more weakly than the substrates.

Pre-Steady-State Kinetics of B. anthracis OSB-CoA Synthetase Reacting with ATP and OSB in the First Half-Reaction. The production and release of PP_i were observed for the OSB-CoA synthetase half-reaction with ATP and OSB as substrates in the absence of CoA. To measure the rate of PP_i production in the absence of CoA, the phosphate detection assay was utilized to monitor the increase in the concentration of PP_i over time and at several high concentrations of the enzyme ($[E]_t$ = 2.2, 4.4, and 8.8 μM) in the presence of saturating amounts of ATP (512 μM) and OSB (256 μM). The results of these studies are presented in Figure 5. The time courses for PP_i production were fit to eq 12, and the values of the pre-steady-state kinetic parameters are summarized in Table 3. A set of distinct, biphasic curves was obtained whereby a fast burst phase is followed by a slower and linear steady-state phase. The magnitude of the observed burst amplitudes for the curves in Figure 5, which are proportional to the concentration of PP_i produced, closely approached the concentrations of the enzyme utilized in the experiments (Table 3). A flat line was observed for the experiment with E and ATP, suggesting that no PP_i release occurred without the addition of OSB. These results indicate that the burst phase corresponds to a single-turnover event of the first half-reaction. The observed burst rate constant (k_1) obtained from those curves was approximately 3 times greater than the observed steady-state rate constant ($k_2/[E]_t$). The rate constants of the burst stage ($\sim$4 min^{-1}) and the following steady-state linear stage ($\sim$1 min^{-1}) determined in the absence of CoA were approximately 37 and 142 times lower, respectively, than the steady-state rate constant determined in the presence of CoA ($\sim$155 min^{-1}). These results suggest that CoA influences the rate constants associated with the first half-reaction.

Inhibition Kinetics of TFMP-butyl-AMS. Collectively, the kinetic studies support a bi uni uni bi ping-pong reaction mechanism for *B. anthracis* OSB-CoA synthetase with the formation of an OSB−AMP reaction intermediate. We therefore hypothesized that compounds that mimic the OSB-AMP intermediate may exhibit potent inhibitory effects on the enzyme reaction. To test this hypothesis, a TFMP-butyl-AMS inhibitor (compound **6** in Figure 1) was synthesized by covalently linking compound **5** (Figure 1) and a sulfonamide adenosine to mimic the OSB-AMP intermediate. The inhibition of OSB-CoA synthetase by TFMP-butyl-AMS against each of the three substrates was then probed to determine inhibition mechanisms. Nonlinear regression was performed on the inhibition kinetic data using eqs 8−11, and the resulting goodness-of-fit values for each equation are summarized in Table S3 of the Supporting Information.

When CoA concentrations were varied at fixed concentrations of the inhibitor with ATP and OSB concentrations fixed at subsaturating levels, the data were best fit to eq 9. The Lineweaver−Burk plot of the data produced a series of parallel lines (Figure 6A), indicating that TFMP-butyl-AMS is an uncompetitive inhibitor of CoA. When ATP concentrations were varied at fixed concentrations of the inhibitor with both CoA and OSB concentrations held at subsaturating levels, the data were best fit to eq 10 (Figure 6B), indicating that TFMP-butyl-AMS is a mixed-type inhibitor respect to ATP. When OSB concentrations were varied at fixed concentrations of the inhibitor with both ATP and CoA fixed at subsaturating levels, the data were best fit to eq 10, indicating that mixed-type inhibition with respect to OSB is also observed (Figure 6C). These kinetic patterns of inhibition are in agreement with an ordered bi uni uni bi ping-pong mechanism. The resulting kinetic constants for this study are summarized in Table 2. The inhibitor has αK_i and K_i values in the lower micromolar range compared to AMP and benoyl-CoA, which only have millimolar inhibition values.

DISCUSSION

Studies on OSB-CoA synthetases from *E. coli* and *Mycobacterium phli* suggest that both the aromatic carboxylate group and the aliphatic carboxylate group, especially the linker length, are important for OSB substrate reactivity (*9, 27*). Our data indicate that the linker length of the aliphatic carboxylate group is critical for OSB substrate recognition by *B. anthracis* OSB-CoA synthetase. OSB-CoA synthetase was also found to exhibit moderate selectivity for the

Table 3: Kinetic Parameters Obtained from the Pre-Steady-State Studies of *B. anthracis* OSB-CoA Synthetase

parameter	2.2 μM enzyme[a]	4.4 μM enzyme[a]	8.8 μM enzyme[a]	mean $\pm$ standard deviation[b]
burst amplitude A (μM)	2.0 ± 0.1	4.8 ± 0.1	10.3 ± 0.2	−
burst rate constant k_1 (min^{-1})	3.6 ± 0.5	3.9 ± 0.3	3.9 ± 0.2	3.9 ± 0.6
linear rate constant $k_2/[E]_t$ (min^{-1})	1.2 ± 0.05	1.0 ± 0.05	1.1 ± 0.2	1.1 ± 0.2

[a] Data presented as means $\pm$ the standard error. [b] The mean and standard deviation of three numbers $a \pm \sigma_a$, $b \pm \sigma_b$, and $c \pm \sigma_c$ were calculated as $(a + b + c)/3$ and $(\sigma_a^2 + \sigma_b^2 + \sigma_c^2)^{1/2}$, respectively.

aromatic carboxylate group of OSB: a replacement of the aromatic carboxylate with a CF_3 group results in a viable but less efficient substrate.

The initial velocity, product inhibition, and direct binding studies of *B. anthracis* OSB-CoA synthetase are consistent with an ordered bi uni uni bi ping-pong mechanism with the ordered addition of the first two substrates, ATP followed by OSB, and the ordered release of the last two products, OSB-CoA followed by AMP. On the basis of this kinetic mechanism, the reaction includes two half-reactions, where the enzyme first reacts with ATP and OSB to form PP_i and OSB-AMP and then OSB-AMP reacts with CoA to form OSB-CoA and AMP. Therefore, OSB-CoA synthetase can be classified as a member of the acyl-AMP-forming family of enzymes. Although we do not have direct experimental evidence of the formation of an OSB-AMP intermediate during the reaction, indirect evidence supports the formation of the OSB-AMP intermediate. First, the bi uni uni bi ping-pong mechanism suggests the formation of an OSB-AMP intermediate. Second, the pre-steady-state kinetics of the first half-reaction suggests the presence of a rate-limiting step which is likely the slow release of a tightly bound OSB-AMP intermediate from the active site. Finally, the formation of an acyl-AMP intermediate has been characterized in several members of the acyl-AMP-forming family of enzymes, including acetyl-CoA synthetase (*28*), malonyl-CoA synthetase (*14*), and 4-chlorobenzoate-CoA synthetase (*29*).

It has been observed that acyl-AMP intermediates are capable of binding to their target enzymes between 2 and 3 orders of magnitude tighter than their carboxylate and ATP substrates (*30, 31*). Various nonhydrolyzable acyl-AMP analogues have been synthesized for different enzymes of this family. For instance, salicyl-AMS was found to be a potential inhibitor of *Mycobacterium tuberculosis* enzyme MbtA and *Yersinia pestis* enzyme YbtE, both of which belong to the acyl-AMP-forming family of enzymes involved in the bacterial siderophore biosynthesis (*19*). We therefore designed and synthesized a chemically stable OSB-AMP analogue, TFMP-butyl-AMS (compound **6** in Figure 1), by covalently linking compound **5** (Figure 1) with a sulfonamide adenosine moiety.

The resulting analogue is predicted to be able to occupy the ATP site via its "AMS" portion and the OSB site via its "TFMP-butyl" portion. Since the enzyme follows an ordered mechanism for ATP and OSB binding, it is expected that TFMP-butyl-AMS can bind to the free enzyme as a competitive inhibitor of ATP and a mixed-type inhibitor of OSB. However, TFMP-butyl-AMS exhibited mixed-type inhibition of both ATP and OSB (Figure 6B,C), suggesting that it can bind to the ATP and OSB sites of the free enzyme as well as to the OSB site in the enzyme−ATP complex using its TFMP-butyl portion in an ordered mechanism. Our observation that the affinity of TFMP-butyl-AMS for the enzyme−ATP complex ($\alpha K_i = 108 \pm 17.0$ μM) is comparable to the affinity of compound **5** (the TFMP-butyl portion of the inhibitor) for the enzyme−ATP complex ($K_m = 168 \pm 18.0$ μM) further supports this model. In addition, our observation that TFMP-butyl-AMS is an uncompetitive inhibitor of CoA (Figure 6A) is consistent with this binding model. As expected, the affinity of TFMP-butyl-AMS for the enzyme−ATP complex ($\alpha K_i = 108.0 \pm 17.0$ μM) is much lower than that of the free enzyme ($K_i = 5.2 \pm 0.8$ μM). To the best of our knowledge, this is the first reaction intermediate analogue against OSB-CoA synthetase from any organism with low, micromolar inhibition constants. Unfortunately, the TFMP-butyl-AMS inhibitor was found to have limited whole cell activity against the *B. anthracis* ΔANR strain, presumably due to poor penetration through the cell wall (data not shown).

Several members of the acyl-CoA synthetase subfamily of enzymes utilize bi uni uni bi ping-pong mechanisms (*13, 14, 32, 33*). Interestingly, there are significant differences among those enzymes in terms of the order of addition of the first two substrates and the order of release of the last two products. OSB-CoA synthetase from *B. anthracis* shares a very similar kinetic mechanism with *Bradyrhizobium japonicum* malonyl-CoA synthetase (*14*) and bovine liver medium-chain fatty acid-CoA synthetase (*32*). Their reaction mechanisms all proceed with an ordered addition of the first two substrates and an ordered release of the last two products. The kinetic mechanism of pig liver bile acid-CoA synthetase, however, contains the random release of the last two products (*33*), while yeast acetyl-CoA synthetase follows random addition of the first two substrates and random release of the last two products (*13*).

We have found that CoA is not absolutely required for the production and release of PP_i and OSB-AMP in the first half-reaction. The results of the pre-steady-state kinetic studies indicate that in the absence of CoA, OSB-CoA synthetase reacts with ATP and OSB in a biphasic manner characterized by a burst phase with a rate constant ~3 times greater than that of the following linear, steady-state phase (Figure 5 and Table 3). The burst kinetics suggests that a rapid step in catalysis is followed by a slower step. Our interpretation of these data is that in the first phase of the half-reaction, ATP and OSB combine with the enzyme and react rapidly to form OSB-AMP and PP_i. Because the assay we routinely utilize detects the formation of PP_i, the more rapid initial step would represent the formation and release of PP_i. In the second and slower linear phase of the first half-reaction, OSB-AMP is released slowly from the enzyme−OSB-AMP complex to regenerate the free enzyme for a second round of turnover. The difference in rate constant for these two steps in the absence of CoA is approximately 3−4-fold. Thus, for the first half-reaction in the absence of CoA, the slow release of OSB-AMP (1 min^{-1})

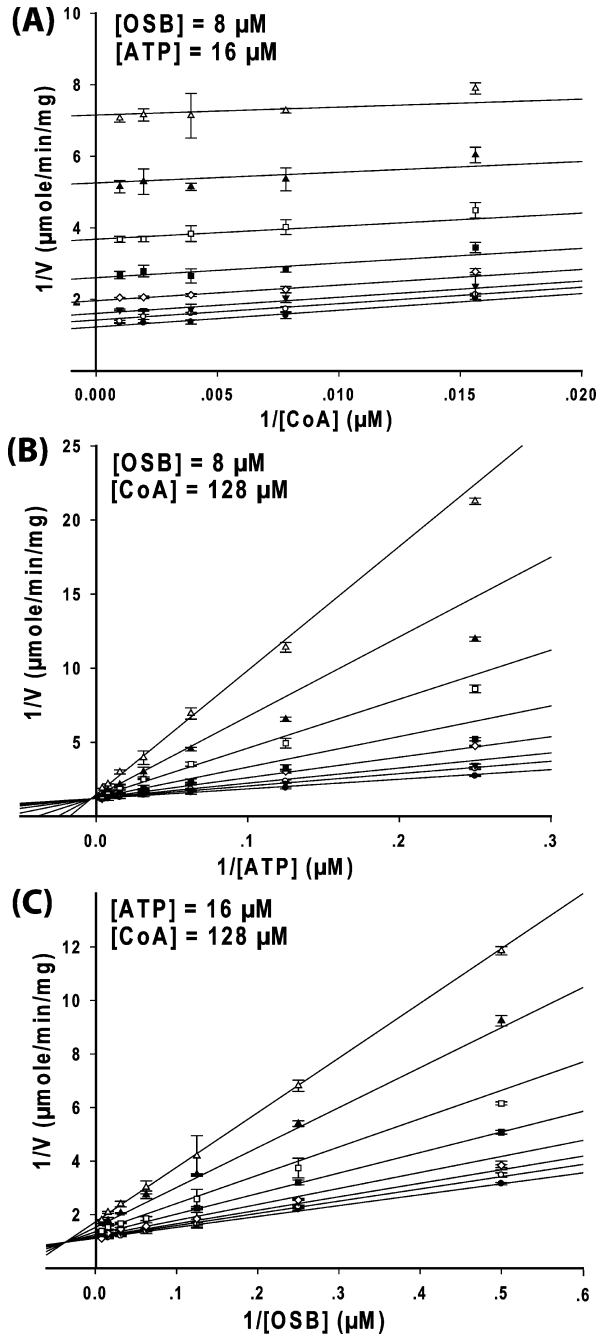

FIGURE 6: Inhibition study of TFMP-butyl-AMS on *B. anthracis* OSB-CoA synthetase activity. The kinetic data were displayed as Lineweaver−Burk plots of the reaction rate vs substrate concentrations at different inhibitor concentrations. For each plot, the levels of two substrates were kept constant while the levels of the third substrate and the inhibitor were varied. (A) Uncompetitive inhibition of CoA. The OSB and ATP concentrations were kept constant at 8 and 16 μM, respectively, while the CoA and inhibitor concentrations were varied: (●) 0, (○) 1.56, (▼) 3.13, (◇) 6.25, (■) 12.5, (□) 25, (▲) 50, and (△) 100 μM. (B) Mixed-type inhibition of ATP. The OSB and CoA concentrations were kept constant at 8 and 128 μM, respectively, while the ATP and inhibitor concentrations were varied: (●) 0, (○) 1.56, (▼) 3.13, (◇) 6.25, (■) 12.5, (□) 25, (▲) 50, and (△) 100 μM. (C) Mixed-type inhibition of OSB. The ATP and CoA concentrations were kept constant at 16 and 128 μM, respectively, while the OSB and inhibitor concentrations were varied: (●) 0, (○) 0.78, (▼) 1.56, (◇) 3.13, (■) 6.25, (□) 12.5, (▲) 25, and (△) 50 μM. Each data point represents the mean of a duplicate test. The upper and lower bars represent the duplicate measurements. The kinetic parameters and patterns are summarized in Table 2.

from the active site most likely represents the rate-limiting step compared to the production and release of PP_i in the first turnover of ~4 min^{-1} (Scheme 2A).

When the OSB-CoA synthetase reaction is performed in the presence of CoA, the turnover number, k_{cat}, as determined via the phosphate detection assay, is approximately 155 min^{-1} which is approximately 147-fold faster than the steady-state rate for the first half-reaction (1.1 min^{-1}) in the absence of CoA (Scheme 2A,B). This value is nearly identical to the k_{cat} value of 134 min^{-1} for the overall reaction as determined by the direct detection of the final product, OSB-CoA (Scheme 2B). The increase in the rate of the first half-reaction in the presence of CoA would suggest that CoA must somehow bind to the enzyme during the first half-reaction or immediately at the time of OSB-AMP and PP_i formation and/or release. From a simplistic view of kinetic schemes, this would at first seem to conflict with a bi uni uni bi ping-pong mechanism; i.e., the third substrate always binds to the enzyme after the first half-reaction. In the case of OSB-CoA synthetase, this would require that OSB-AMP and PP_i be formed and PP_i be released before the binding of CoA. Our data strongly support the bi uni uni bi ping-pong mechanism, but the interesting observation of the rate acceleration of the first half-reaction by CoA requires further mechanistic exploration into potential explanations for this phenomenon.

Our first avenue of exploration was to examine the existing literature on enzymes that catalyze reactions similar to OSB-CoA synthetase as well as utilize bi uni uni bi ping-pong kinetic mechanisms. The enzyme pantothenate synthetase from *M. tuberculosis* (*Mt*PS) catalyzes a bi uni uni bi ping-pong reaction in its transformation of ATP, pantoate, and β-alanine into PP_i, pantothene, and AMP, respectively (*15*). In a series of steady-state and pre-steady-state kinetic studies on *Mt*PS, Zheng and Blanchard demonstrated that in the absence of the third substrate, β-alanine, the rate of PP_i formation and release for the first half-reaction is 1.3 s^{-1}. However, in the presence of β-alanine, the rate increases to 1.8 s^{-1} as measured by the production of PP_i, or to 3.4 s^{-1} as measured by the formation of AMP (*15*). These results suggest that β-alanine is somehow capable of increasing the rate of the first half-reaction, although it is predicted to bind only after the release of PP_i. Unfortunately, further experimental studies or hypotheses to explain these observations have not yet been published.

The enzyme 4-chlorobenzoyl-CoA ligase (4CBA:CoA ligase) from *Pseudomonas* sp. strain CBS3 catalyzes the transformation of 4-chlorobenzoate (4-CBA), ATP, and CoA into PP_i, 4-CBA-CoA, and AMP (*29*). In a series of steady-state and pre-steady-state kinetic studies, Dunaway-Mariano and co-workers observed that the rate of production and release of PP_i for the first half-reaction, the conversion of 4-CBA and ATP into 4-CBA-AMP and PP_i, is 0.013 s^{-1} in the absence of CoA. In the presence of CoA, however, the rate increases ~3000-fold to 40 s^{-1} (*29*). During the course of the reaction, the production of the intermediate, 4-CBA-AMP, was confirmed and its rate of formation measured (*29*). Unfortunately, it was not established in those studies whether 4CBA:CoA ligase utilizes a bi uni uni bi ping-pong mechanism. Subsequent experiments to do so have not yet been performed (D. Dunaway-Mariano, personal communication).

Scheme 2

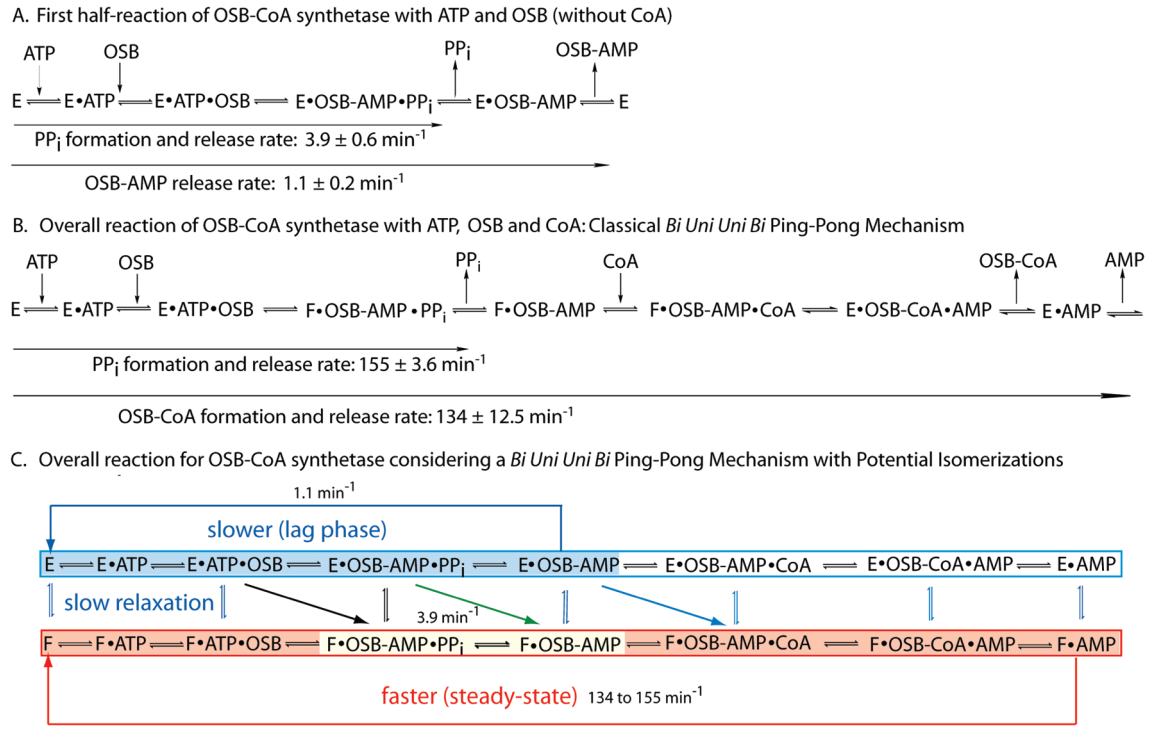

Recent and extensive steady-state and pre-steady-state kinetic studies, in conjunction with X-ray structural studies, have been performed by the Dunaway-Mariano group on 4CBA:CoA ligase isolated from *Alcaligenes* sp. strain AL3007 (*34, 35*). From their kinetic studies, it was rigorously established that 4CBA:CoA ligase utilizes a bi uni uni bi ping-pong kinetic mechanism and that PP_i release must precede CoA binding (*35*). Interestingly, they found that the overall reaction is characterized by a burst phase in the production of the product 4-CBA-CoA (60 s^{-1}) followed by a slower steady-state rate (10.2 s^{-1}). These data suggest that a step after the formation of the product 4-CBA-CoA is rate-determining. To help further establish the mechanism for the rate-limiting step, the X-ray structures of two 4CBA:CoA ligase complexes, one with the reaction intermediate 4-CB-AMP bound and the other with both AMP and 4-CP-CoA bound, were determined (*34*). The structural data suggested that 4CBA:CoA ligase undergoes a significant conformational change in transforming between the 4-CB-AMP complex (designated conformer 2) and the substrate-bound or 4-CB-AMP-Mg-PP_i-bound complex (designated conformer 1). The slow rate of isomerization of conformer 2 back to conformer 1 is proposed to be the rate-limiting step in the 4CBA:CoA ligase kinetic mechanism (*35*). This step is indicated in by the green diagonal arrow in Scheme 2C in an analogous position of our proposed reaction scheme for OSB-CoA synthetase.

The observation of a rate-limiting, conformational change in the 4CBA:CoA ligase-catalyzed reaction, described as a "domain alteration" mechanism (*36*), provides a compelling model that may apply to the OSB-CoA synthetase mechanism. By combining parts A and B of Scheme 2 and then introducing potential conformational isomerization events between the various enzyme forms E and F that could occur along the reaction pathway, we propose a more general bi uni uni bi isomerization (iso) ping-pong mechanism (Scheme 2C) that we believe applies to OSB-CoA synthetase specifically, and potentially to many other enzymes such as 4CBA:CoA ligase in general.

In the model proposed in Scheme 2C, in the absence of CoA, OSB-CoA synthetase could catalyze the first half-reaction solely with complexes involving enzyme form E that are catalytically less active than complexes involving enzyme form F. This path is indicated in Scheme 2A and would be considered a nontraditional ping-pong mechanism since it does not involve transformation to an F form of the enzyme. It is also possible that in the absence of CoA, OSB-CoA synthetase could catalyze the first half-reaction in the classical ping-pong mechanism by converting the ternary E•ATP•OSB complex directly to the F•OSB-AMP•PP_i complex (represented by the black diagonal arrow in Scheme 2C) which would then release the product PP_i forming the F•OSB-AMP complex (yellow box in Scheme 2C). The k_{cat} value of 3.9 min^{-1} would apply to this path. The F•OSB-AMP complex could then slowly isomerize back to an E•OSB-AMP complex which would then release OSB-AMP from E for another round of catalytic turnover at a rate of 1.1 min^{-1}.

In the presence of CoA, once PP_i is released from the F•OSB-AMP•PP_i complex, CoA could rapidly combine with the F•OSB-AMP complex to then complete the formation and release of products from the F enzyme complexes (indicated by the red shaded box in Scheme 2C). Once the free enzyme, F, is released at the end of this first reaction

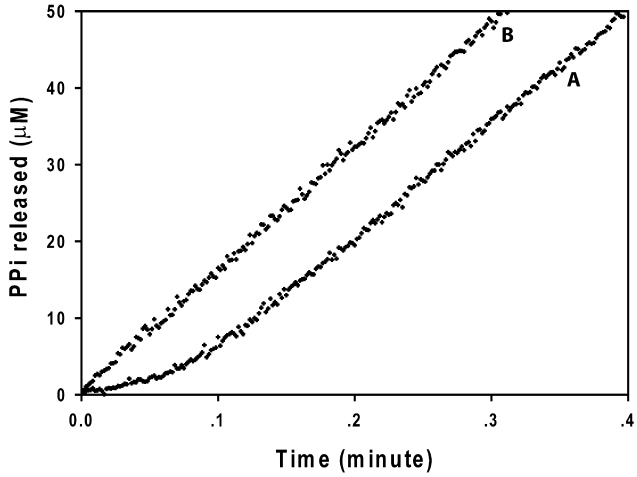

FIGURE 7: Plot of PP_i released as a function of time in the overall reaction of *B. anthracis* OSB-CoA synthetase. In plot A, OSB-CoA synthetase was mixed with 256 μM OSB, 512 μM ATP, 1024 μM CoA, and 2 mM $MgCl_2$ and the release of PP_i was monitored using the phosphate detection assay. The absorbance at 360 nm was converted into the amount of PP_i released using a molar extinction coefficient of 11000 M^{-1} cm^{-1}. A lag phase followed by a linear steady state was observed for plot A. In plot B, OSB-CoA synthetase was first preincubated with 256 μM OSB, 512 μM ATP, and 2 mM $MgCl_2$ for 1 min; a final CoA concentration of 1024 μM was then added, and the release of PP_i was monitored. A linear steady-state curve without a lag phase was observed for plot B. To ensure that the observed lag phase was not due to any inherent lag phase of the coupled assay, an excess of the coupling enzymes was added such that the inherent, theoretical lag phase would be at most 0.12 s (see Calculation of the inherent lag phase (τ) of the coupled assay in the pre-steady-state kinetic studies of E+ATP+OSB+CoA of the Supporting Information). The lack of an observed lag phase in Figure 5 also supports the possibility that the observed lag phase is associated with the isomerization of OSB-CoA synthetase.

cycle, it would rapidly combine with substrates, ATP followed by OSB, to form the F·ATP·OSB complex that would then proceed to generate products. The overall rate of 134−155 min^{-1} would then apply to each round of the subsequent catalytic turnovers in the steady state. The isomerization of free F back to free E would be slow compared to the formation of the F·ATP·OSB complex. This model would explain the kinetic results for the OSB-CoA synthetase reaction described above.

The model proposed in Scheme 2C would also then predict that a lag phase may exist in the time course of the OSB-CoA synthetase-catalyzed reaction. We therefore carefully performed a cuvette-based assay to more accurately assess the presence of any lag phase. In the presence of saturating concentrations of ATP, OSB, and CoA, a lag phase is clearly evident within the first few seconds of the reaction (Figure 7) that supports a bi uni uni bi iso ping-pong mechanism in which the rate of formation of the F·OSB-AMP complex from free E is slow in the initial turnovers of the enzyme, but once the enzyme complexes involving the F forms of the enzyme are produced, they are maintained during the steady-state turnover of the enzyme. Although the lag phase lends support to the idea that the F·OSB-AMP complex is produced, it does not rule out the possibility that CoA combines directly with the E·OSB-AMP complex to then produce the F·OSB-AMP·CoA complex (blue diagonal arrow in Scheme 2C).

To determine which of the complexes (E·OSB-AMP or F·OSB-AMP) CoA combines most readily, we incubated OSB-CoA synthetase with saturating levels of ATP and OSB in the absence of CoA to attain the steady-state rate for the first half-reaction. We then initiated the second half-reaction by the addition of a saturating concentration of CoA to check for any lag phase before the steady-state phase of the overall reaction is achieved. The progress curve data in Figure 7 clearly indicate that the lag phase for the reaction has been abolished. This observation supports a mechanism in which the F·OSB-AMP complex is generated and stabilized via the first half-reaction, and in the absence of CoA, it slowly isomerizes back to the E·OSB-AMP complex releasing the intermediate. When CoA is present, it readily combines with the F·OSB-AMP complex to complete the reaction cycle via the F form enzyme complexes. Had a lag phase also been observed upon the addition of CoA, it would have suggested that the F·OSB-AMP-CoA complex is formed directly from the E·OSB-AMP complex (indicated by the blue diagonal arrow), but this is not the case for OSB-CoA synthetase.

In conclusion, the essential nature of menaquinone biosynthesis for the survival of bacteria and the lack of this pathway in humans suggest that enzymes in this pathway may be potential targets for the discovery of antibiotics. This is the first report of the kinetic mechanism of OSB-CoA synthetase, a key enzyme for bacterial menaquinone biosynthesis. The formation of the OSB-AMP intermediate in the OSB-CoA synthetase-catalyzed reaction, as suggested by our kinetic mechanism, as well as our data on TFMP-butyl-AMS, indicates that structural homologues of OSB-AMP can function as potential inhibitors of this enzyme. The ordered bi uni uni bi iso ping-pong reaction mechanism proposed for the OSB-CoA synthetase reaction is a subset of a potentially more universal kinetic scheme for this class of enzymes and others that catalyze similar reactions. The prediction of conformational isomerizations along the reaction pathways of enzymes that utilize bi uni uni bi ping-pong mechanisms will help to provide a mechanistic framework by which explanations can be provided to explain the different lag and burst phases associated with different steps of the reaction. The conformational isomerziation model also helps to explain how OSB-CoA synthetase accommodates two half-reactions using the same active site during the reaction. We are currently attempting to obtain the X-ray crystal structure of OSB-CoA synthetase in complex with various substrates, products, and reaction intermediate mimics to reveal the structural mechanisms and isomerizations predicted for this two-half-reaction mechanism.

SUPPORTING INFORMATION AVAILABLE

Methods for the cloning, overexpression, and purification of $(His)_6$-tagged *E. coli* 1,4-dihydroxy-2-naphthoate-CoA (DHNA-CoA) synthetase, syntheses of compounds **1**−**6**, determination of the pH optimum and data on the effect of Mg^{2+} on *B. anthracis* OSB-CoA synthetase activity, calculation of the inherent lag phase (τ) of the coupled assay in the pre-steady-state kinetic studies of the E + ATP + OSB + CoA reaction, goodness-of-fit information for the experimental data for various equations in the bisubstrate initial velocity studies, and schematics of the coupled enzyme assays utilized for the detection of *B. anthracis* OSB-CoA synthetase activity. This material is available free of charge via the Internet at http://pubs.acs.org.

REFERENCES

1. Bentley, R., and Meganathan, R. (1982) Biosynthesis of vitamin K (menaquinone) in bacteria. *Microbiol. Rev. 46*, 241–280.
2. Collins, M. D., and Jones, D. (1981) Distribution of isoprenoid quinone structural types in bacteria and their taxonomic implication. *Microbiol. Rev. 45*, 316–354.
3. Kobayashi, K., Ehrlich, S. D., Albertini, A., Amati, G., Andersen, K. K., Arnaud, M., Asai, K., Ashikaga, S., Aymerich, S., Bessieres, P., Boland, F., Brignell, S. C., Bron, S., Bunai, K., Chapuis, J., Christiansen, L. C., Danchin, A., Debarbouille, M., Dervyn, E., Deuerling, E., Devine, K., Devine, S. K., Dreesen, O., Errington, J., Fillinger, S., Foster, S. J., Fujita, Y., Galizzi, A., Gardan, R., Eschevins, C., Fukushima, T., Haga, K., Harwood, C. R., Hecker, M., Hosoya, D., Hullo, M. F., Kakeshita, H., Karamata, D., Kasahara, Y., Kawamura, F., Koga, K., Koski, P., Kuwana, R., Imamura, D., Ishimaru, M., Ishikawa, S., Ishio, I., Le Coq, D., Masson, A., Mauel, C., Meima, R., Mellado, R. P., Moir, A., Moriya, S., Nagakawa, E., Nanamiya, H., Nakai, S., Nygaard, P., Ogura, M., Ohanan, T., O'Reilly, M., O'Rourke, M., Pragai, Z., Pooley, H. M., Rapoport, G., Rawlins, J. P., Rivas, L. A., Rivolta, C., Sadaie, A., Sadaie, Y., Sarvas, M., Sato, T., Saxild, H. H., Scanlan, E., Schumann, W., Seegers, J. F. M. L., Sekiguchi, J., Sekowska, A., Seror, S. J., Simon, M., Stragier, P., Studer, R., Takamatsu, H., Tanaka, T., Takeuchi, M., Thomaides, H. B., Vagner, V., van Dijl, J. M., Watabe, K., Wipat, A., Yamamoto, H., Yamamoto, M., Yamamoto, Y., Yamane, K., Yata, K., Yoshida, K., Yoshikawa, H., Zuber, U., and Ogasawara, N. (2003) Essential *Bacillus subtilis* genes. *Proc. Natl. Acad. Sci. U.S.A. 100*, 4678–4683.
4. Read, T. D., Peterson, S. N., Tourasse, N., Baillie, L. W., Paulsen, I. T., Nelson, K. E., Tettelin, H., Fouts, D. E., Eisen, J. A., Gill, S. R., Holtzapple, E. K., Okstad, O. A., Helgason, E., Rilstone, J., Wu, M., Kolonay, J. F., Beanan, M. J., Dodson, R. J., Brinkac, L. M., Gwinn, M., DeBoy, R. T., Madpu, R., Daugherty, S. C., Durkin, A. S., Haft, D. H., Nelson, W. C., Peterson, J. D., Pop, M., Khouri, H. M., Radune, D., Benton, J. L., Mahamoud, Y., Jiang, L. X., Hance, I. R., Weidman, J. F., Berry, K. J., Plaut, R. D., Wolf, A. M., Watkins, K. L., Nierman, W. C., Hazen, A., Cline, R., Redmond, C., Thwaite, J. E., White, O., Salzberg, S. L., Thomason, B., Friedlander, A. M., Koehler, T. M., Hanna, P. C., Kolsto, A. B., and Fraser, C. M. (2003) The genome sequence of *Bacillus anthracis* Ames and comparison to closely related bacteria. *Nature 423*, 81–86.
5. Webb, M. R. (1992) A continuous spectrophotometric assay for inorganic phosphate and for measuring phosphate release kinetics in biological systems. *Proc. Natl. Acad. Sci. U.S.A. 89*, 4884–4887.
6. Van Veldhoven, P. P., and Mannaerts, G. P. (1987) Inorganic and organic phosphate measurements in the nanomolar range. *Anal. Biochem. 161*, 45–48.
7. Bodem, G. B., and Leete, E. (1976) Biosynthesis of shihunine in *Dendrobium pierardii*. *J. Am. Chem. Soc. 98*, 6321.
8. Bryant, R. W., Jr., and Bentley, R. (1976) Menaquinone biosynthesis: Conversion of o-succinylbenzoic acid to 1,4-dihydroxy-2-naphthoic acid and menaquinones by *Escherichia coli* extracts. *Biochemistry 15*, 4792–4796.
9. Kwon, O., Bhattacharyya, D. K., and Meganathan, R. (1996) Menaquinone (vitamin K-2) biosynthesis: Overexpression, purification, and properties of o-succinylbenzoyl-coenzyme A synthetase from *Escherichia coli*. *J. Bacteriol. 178*, 6778–6781.
10. Meganathan, R., and Bentley, R. (1979) Menaquinone (vitamin K2) biosynthesis: Conversion of o-succinylbenzoic acid to 1,4-dihydroxy-2-naphthoic acid by *Mycobacterium phlei* enzymes. *J. Bacteriol. 140*, 92.
11. Papas, T. S., and Peterkofsky, A. (1972) A random sequential mechanism for arginyl transfer ribonucleic acid synthetase of *Escherichia coli*. *Biochemistry 11*, 4602–4608.
12. Farrar, W. W., and Plowman, K. M. (1975) Kinetics of acetyl-CoA synthetase-I. Mode of addition of substrates. *Int. J. Biochem. 6*, 537–542.
13. Farrar, W. W., and Plowman, K. M. (1979) Kinetics of acetyl-CoA synthetase-II. Products inhibition studies. *Int. J. Biochem. 10*, 583–588.
14. Kim, Y. S., and Kang, S. W. (1994) Steady-State Kinetics of Malonyl-Coa Synthetase from *Bradyrhizobium japonicum* and Evidence for Malonyl-Amp Formation in the Reaction. *Biochem. J. 297*, 327–333.
15. Zheng, R., and Blanchard, J. S. (2001) Steady-state and pre-steady-state kinetic analysis of *Mycobacterium tuberculosis* pantothenate synthetase. *Biochemistry 40*, 12904–12912.
16. Cohn, M., and Hu, A. (1978) Isotopic (^{18}O) shift in ^{31}P nuclear magnetic resonance applied to a study of enzyme-catalyzed phosphate−phosphate exchange and phosphate (oxygen)−water exchange reactions. *Proc. Natl. Acad. Sci. U.S.A. 75*, 200–203.
17. May, J. J., Kessler, N., Marahiel, M. A., and Stubbs, M. T. (2002) Crystal structure of DhbE, an archetype for aryl acid activating domains of modular nonribosomal peptide synthetases. *Proc. Natl. Acad. Sci. U.S.A. 99*, 12120–12125.
18. Grayson, N. A., and Westkaemper, R. B. (1988) Stable analogs of acyl adenylates. Inhibition of acetyl- and acyl-CoA synthetase by adenosine 5′-alkylphosphates. *Life Sci. 43*, 437–444.
19. Ferreras, J. A., Ryu, J.-S., Lello, F. D., Tan, D. S., and Quadri, L. E. N. (2005) Small-molecule inhibition of siderophore biosynthesis in *Mycobacterium tuberculosis* and *Yersinia pestis*. *Nat. Chem. Biol. 1*, 29.
20. Truglio, J. J., Theis, K., Feng, Y., Gajda, R., Machutta, C., Tonge, P. J., and Kisker, C. (2003) Crystal structure of *Mycobacterium tuberculosis* MenB, a key enzyme in vitamin K2 biosynthesis. *J. Biol. Chem. 278*, 42352–42360.
21. Akaike, H. (1974) A new look at the statistical model identification. *IEEE Trans. Autom. Control 19*, 716–723.
22. Menguy, T., Chenevois, S., Guillain, F., le Maire, M., Falson, P., and Champeil, P. (1998) Ligand binding to macromolecules or micelles: Use of centrifugal ultrafiltration to measure low-affinity binding. *Anal. Biochem. 264*, 141–148.
23. Wolfer, G. K., Jr., and Rippon, W. B. (1987) Protocols for use of ultrafiltration in determination of free ligand concentration and of complexity of ligand/protein interactions. *Clin. Chem. 33*, 115–117.
24. Grant, B. D., and Adams, J. A. (1996) Pre-steady-state kinetic analysis of cAMP-dependent protein kinase using rapid quench flow techniques. *Biochemistry 35*, 2022–2029.
25. Northrop, D. B. (1998) On the meaning of Km and V/K in enzyme kinetics. *J. Chem. Educ. 75*, 1153–1157.
26. Northrop, D. B. (1999) So what exactly is V/K, anyway? In *Biomedical and Health Research* (Frey, P. A., and Northrop, D. B., Eds.) pp 250−263, IOS Press, Amsterdam.
27. Sieweke, H. J., and Leistner, E. (1991) o-Succinylbenzoate: coenzyme A ligase, an enzyme involved in menaquinone (vitamin K2) biosynthesis, displays broad specificity. *Z. Naturforsch. C46*, 585–590.
28. Midelfort, C. F., and Sarton-Miller, I. (1978) The stereochemical course of acetate activation by yeast acetyl-CoA synthetase. *J. Biol. Chem. 253*, 7127–7129.
29. Chang, K. H., and DunawayMariano, D. (1996) Determination of the chemical pathway for 4-chlorobenzoate:coenzyme a ligase catalysis. *Biochemistry 35*, 13478–13484.
30. Kim, S., Lee, S. W., Choi, E. C., and Choi, S. Y. (2003) Aminoacyl-tRNA synthetases and their inhibitors as a novel family of antibiotics. *Appl. Microbiol. Biotechnol. 61*, 278–288.
31. Cassio, D., Lemoine, F., Waller, J. P., Sandrin, E., and Boissonnas, R. A. (1967) Selective inhibition of aminoacyl ribonucleic acid synthetases by aminoalkyl adenylates. *Biochemistry 6*, 827–836.
32. Vessey, D. A., and Kelley, M. (2001) Characterization of the reaction mechanism for the XL-I form of bovine liver xenobiotic/medium-chain fatty acid:CoA ligase. *Biochem. J. 357*, 283–288.
33. Kelley, M., and Vessey, D. A. (1994) Determination of the mechanism of reaction for bile acid: CoA ligase. *Biochem. J. 304*, 945–949.
34. Reger, A. S., Wu, R., Dunaway-Mariano, D., and Gulick, A. M. (2008) Structural characterization of a 140° domain movement in the two-step reaction catalyzed by 4-chlorobenzoate:CoA ligase. *Biochemistry 47*, 8016–8025.
35. Wu, R., Cao, J., Lu, X., Reger, A. S., Gulick, A. M., and Dunaway-Mariano, D. (2008) Mechanism of 4-chlorobenzoate:coenzyme a ligase catalysis. *Biochemistry 47*, 8026–8039.
36. Bandarian, V., Pattridge, K. A., Lennon, B. W., Huddler, D. P., Matthews, R. G., and Ludwig, M. L. (2002) Domain alternation switches B_{12}-dependent methionine synthase to the activation conformation. *Nat. Struct. Biol. 9*, 53–56.

BI801311D